Objective

The aim of this work is to identify and quantify the contribution from the oceanic processes besides the mixed layer process. The Philippine Sea features rich oceanic phenomena with the processes less well represented in the mixed layer model, such as the complex surface current structure, upwelling, and thermocline variation. These oceanic processes have a variability related to El Niño; in order to further predictive skill of sea surface temperature on the interannual time scale in this region, understanding the mechanisms of oceanic variability affecting the sea surface temperature change are critically needed.

Literature

The anomalous sea surface temperature in the Philippine Sea/western Pacific sector tends to be negative during El Niño events (Harrison and Larkin, 1996; Weisberg and Wang, 1997; Klein *et al.*, 1999). In the "western Pacific oscillator" theory proposed by Weisberg and Wang (1997), the sea surface temperature fluctuations in the western Pacific sector serve as the main trigger for the ENSO oscillations as the cooling of the ocean would generate local positive sea level pressure, thus initiating equatorial easterly winds in the western Pacific and eventually leading to the ENSO turnabout. Within the recent last decade, the sea surface temperature variation in the western Pacific sector has drawn intensive attention for its impact on the regional climate (Hsu *et al*, 2001;Su *et al*, 2002; Wang *et al*, 2000, 2003). A dipole of sea surface temperature anomaly, i.e., the anomalous warming in the South China Sea/marine East Asia and cooling in the Philippine Sea region, is noted to be linked with the near surface atmospheric anticyclonic circulation anomaly east of the Philippines (the so-called "PSAC", Philippine Sea Anticyclone) in introducing a weak East Asia-Pacific teleconnection pattern (Hsu et. al., 2001; Watanabe and Jin, 2002;Wang et. al., 2003). The presence of the PSAC during El Niño winters alters the prevailing North-East monsoon and therefore impacts on the winter surface air temperature in East Asia, including Taiwan.

These findings suggested that the local air-sea interaction feedback is potent in this region (Wang

et al., 2001; Hsu et al., 2001). It is proposed that the increase in evaporation cooling associated with the presence of the anomalous atmospheric anticyclone during the El Niño winter leads to cold sea surface temperature anomalies in the Philippine Sea, in turn the oceanic anomalies feedback on the overlying atmospheric circulation. The wind-evaporation-sea surface temperature (WES) feedback (Xie and Philander, 1994) is demonstrated in the composite figure during the months of October, November and December, when the atmospheric anticyclone anomaly straddling the Philippine Sea and South China Sea appears, causing warming(cooling) in the South China Sea(Philippine Sea) (Wang et al., 2003) (Figure 1).

The formation of the anomalous cooling in the Philippine Sea during El Niño events, however, is considered to be associated with oceanic process (Klein *et al.*, 1999; Chou et al. 2004). Since the GFDL AGCM + mixed layer ocean model capable of depth variation (Lau and Nath, 2003) is able to reproduce the cooling in the Philippine Sea region, we can infer that the mixed layer process, the vertical entrainment process in particular, is important for producing cooling in this region. However, the weaker than the observed cooling in GFDL's simulation also suggests that there are oceanic dynamical processes essential for the quantitative change in the sea surface temperature.

Method

The approach we adopt is to analyze the ocean model results to provide a comprehensive description of the ocean state for the composite of 14 El Niño events during 1955-2003 period. The three-dimensional OGCM data "OFES" (OGCM for the Earth Simulator) and the climate system forecast reanalysis data "CFSR" are used. The current work quantifies the surface forcing as well as oceanic contributions to the upper ocean heat budget in this event by performing heat budget analysis.

In order to improve the understanding of sea surface temperature development in this area, Seasonal-reliant Empirical Orthogonal Function (S-EOF) analysis (Wang and An, 2005) is conducted, whereby the fundamental physics of the sea surface temperature evolution is to be studied.

Results and Discussions

I. SSTA evolution

Concurrent with most large El Niño events, cold sea surface temperature anomalies are observed over the western Pacific region. The composite SSTA of 14 El Niño events during 1955-2003 period reveals that there are two stage development of sea surface temperature cooling during the El Niño: the first peak of cooling appears in August-September of Nino(0) year, while the second peak in January-February of Nino(1) year (as shown in Figure 2). The OFES results show similar two stage SST cooling, but the second cooling in January-February of Nino(1) year appears much weaker (Figure 3).

Figure 4 indicates that the WES feedback is the dominate mechanism for the SST cooling in January-February of Nino(1): the high wind therefore the enhanced evaporation cooling result in cooler SST. In August-September of Nino(0), the SST cools while the total wind speed is weak, suggesting that the WES mechanism is not responsible for the first stage of SST cooling

II. Heat budget Analysis

Figure 5 shows the monthly composite of mixed layer heat budget in the Western Pacific region (140° E-170° E, 2° N-13° N) from OFES model data. The heat budget was calculated based on the mixed layer budget method using level-coordinate model as described in Kim et al. (2005). In Kim et al. (2005) paper, the entrainment heat advection is found to be an important component in subsurface process contributing to SST change. In Figure 5, it is seen that the entrainment cooling becomes big in the spring of Nino(1). The upwelling cooling term ($w \, dT/dz$) has a contribution to SST cooling during the whole El Niño developing year and becomes largest in November, but its contribution minimized in the spring of Nino(1). The heat budget analysis from the model also shows that the SST change basically follow the variation of heat flux. The ocean advection serves as a big component in ocean dynamics contributes to the SST variation. For the first sea surface temperature cooling, the advection term is negative contribution; however, during the second sea surface temperature cooling phase the advection term becomes strong positive contribution. During the second cooling phase, the surface thermal forcing

(heat flux), however, turns into a negative contributor; it should be related to the enhanced latent heat cooling due to the existence of PSAC.

The result indicates that MLD mixing, the tendency due to the mixing within the mixed layer, representing the GM mixing and the KPP nonlocal component from the model, should the dominant term for the second SST cooling (as it needs a large residual term to compensate the positive advection) while the subsurface process, including entrainment and upwelling cooling, work together with the ocean advection for the cause of the first stage of cooling.

III. S-EOF results

In order to improve the understanding of sea surface temperature development in this area, Seasonal-reliant Empirical Orthogonal Function (S-EOF) analysis (Wang and An, 2005) is conducted. Figure 6 and 7 show the first three EOF modes of variability for yearly SST evolution over the western Pacific region (130° E-180° E, 0° N-15° N). The second mode (about 20% of total variance) is associated with Nino 3 and Nino 3.4 by one year lag, with EMI (Ashok et al., 2007) both by zero and one year lag. It is not clear yet what the first and third modes of EOF analysis are related to, but all EOF modes appear not to be associated with PDO (Table 1). The results of S-EOF indicate that SST variability in the western Pacific region is complicated and not clearly identified yet, and that there are only 20% variance related to ENSO.

References

Chou, S.-H.; Chou, M.-D.; Chan, P.-K.; Lin, P.-H.; Wang, K.-H. (2004), Tropical Warm Pool Surface Heat Budgets and Temperature: Contrasts between 1997/98 El Niño and 1998/99 La Nina. J. Climate, 17, 1845-1858.

Harrison, D.E., and N.K. Larkin (1996), The COADS sea level pressure signal: A near-global El Niño composite and time series view, 1946-1993. *J. Climate*, **9 (12)**, 3025-3055.

Hsu, H.-H, Y.L. Chen, and W.S. Kau (2001), Effects of Atmosphere-Ocean Interaction on the Interannual Variability of Winter Temperature in Taiwan and East Asia. *Climate Dynamics*, **17**, 305-316.

Klein, S. A., B. J. Soden, and N. -C. Lau (1999), Remote sea surface temperature variations during ENSO: Evidence for a tropical Atmospheric bridge. *J. Climate.*, **12,** 917- 932.

Large, W.G., J.C. McWilliams, and S.C. Doney (1994), Oceanic vertical mixing: A review and a model with a vertical K-profile boundary layer parameterization. *Rev Geophys.*, 363-403.

Lau, N.-C., and M. J. Nath (2003), Atmosphere–ocean variations in the Indo–Pacific sector during ENSO episodes. *J. Climate*, **16,** 3–20.

Luo, J.-J., S. Masson, E. Roeckner, G. Madec, and T. Yamagata (2005), Reducing Climatology Bias in an Ocean–Atmosphere CGCM with Improved Coupling Physics. *J. Climate*, **16,** 2344–2360.

Mitchum, G. T., and R. Lukas (1990), Westward propagation of annual sea level and wind signals in the western Pacific Ocean. *J. Climate*, **3,** 1102–1110.

Neelin, J. D., D. S. Battisti, A. C. Hirst, F.-F. Jin, Y. Wakata, T. Yamagata, and S. E. Zebiak (1998), ENSO theory. *J. Geophys. Res.*, **103,** 14 261–14 290.

Sasaki, H., Y. Sasai, S. Kawahara, M. Furuichi, F. Araki, A. Ishida, Y. Yamanaka, Y. Masumoto, and H. Sakuma (2004), A series of eddy-resolving ocean simulations in the world ocean —OFES (OGCM for the Earth Simulator) project— Proc. OCEANS'04 MTS/IEEE TECHNO-OCEAN'04, 3, 1535–1541.

Sasaki, H., Y. Sasai, M. Nonaka, Y. Masumoto, and S. Kawahara (2006), An eddy-resolving simulation of the quasi-global ocean driven by satellite-observed wind field: Preliminary outcomes from physical

and biological fields. J. Earth Simulator, **6,** 35–49.

Su, H., J. D. Neelin, and C. Chou (2002), Tropical teleconnection and local response to SST anomalies during 1997 – 1998 El Niño, *J. Geophys. Res.*, **106**, 20,025–20,043, 2001.

Wang, B., R. Wu, and T. Li (2003), Atmosphere-Warm Ocean interaction and its impact on Asian-Australian Monsoon variation. *J. Climate.*, **16,** 1195-1211.

Wang, B., R. Wu, and X. Fu (2000), Pacific-East Asian teleconnection: How does ENSO affect East Asian climate? *J. Climate.*, **13**, 1517-1536.

Wang B. and S-I An, 2005: A method for detecting season-dependent modes of climate variability: S-EOF analysis. *Geophys. Res. Lett.*, **32**, L15710.

Weisberg, R. H., and C. Wang (1997), A western Pacific oscillator paradigm for the El Niño–Southern Oscillation. *Geophys. Res. Lett.*, **24,** 779–782.

White, W.B. and R.L. Bernstein (1979), Design of an oceanographic network in the mid-latitude North Pacific. *J. Phys. Oceanogr*., **9**, 592-606.

Wyrtki, K. (1974), Equatorial currents in the Pacific 1950 to 1970 and their relations to the trade winds. *J. Phys. Oceanogr.*, **4**, 372-380.

Xie, S.-P., A. Kubokawa and K. Hanawa (1989), Oscillations with two feedback processes in a coupled ocean-atmosphere model. *J. Climate*, **2**, 946-964.

Xie, S.-P.and S.G.H. Philander, 1994: A coupled ocean-atmosphere model of relevance to the ITCZ in the eastern Pacific. *Tellus*, 4**6A**, 340-350.

Figures

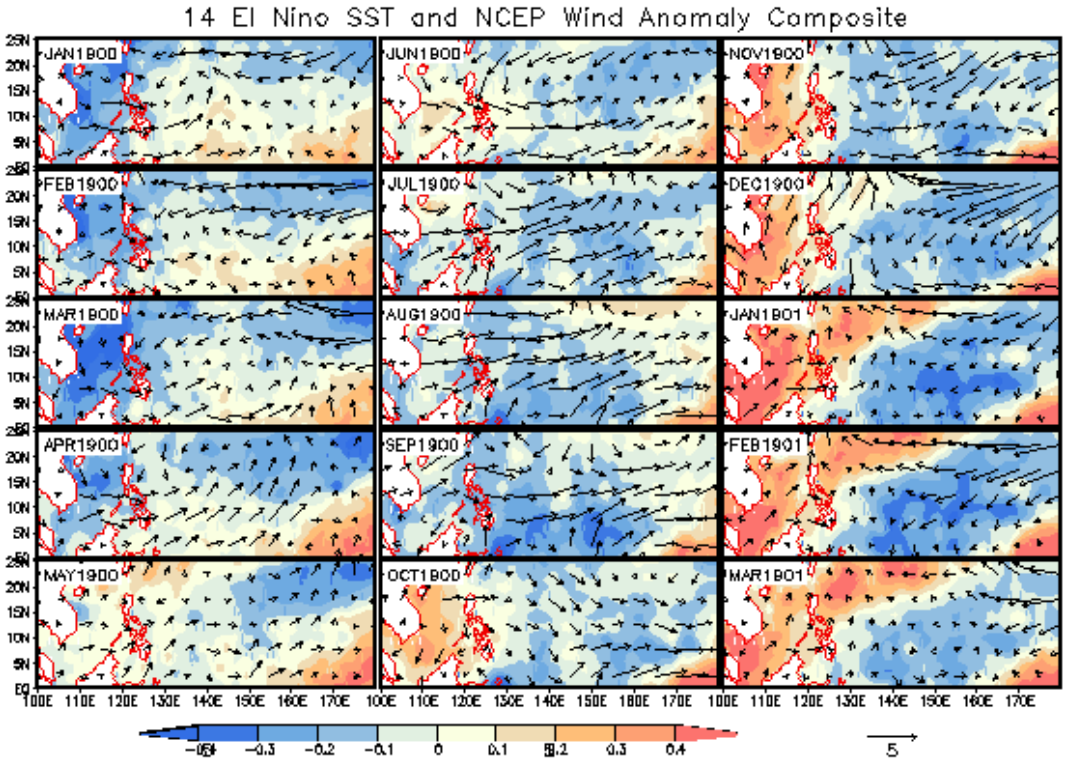

Figure 1. Data Source: HADISST 1.1 and NCEP Reanalysis v2.

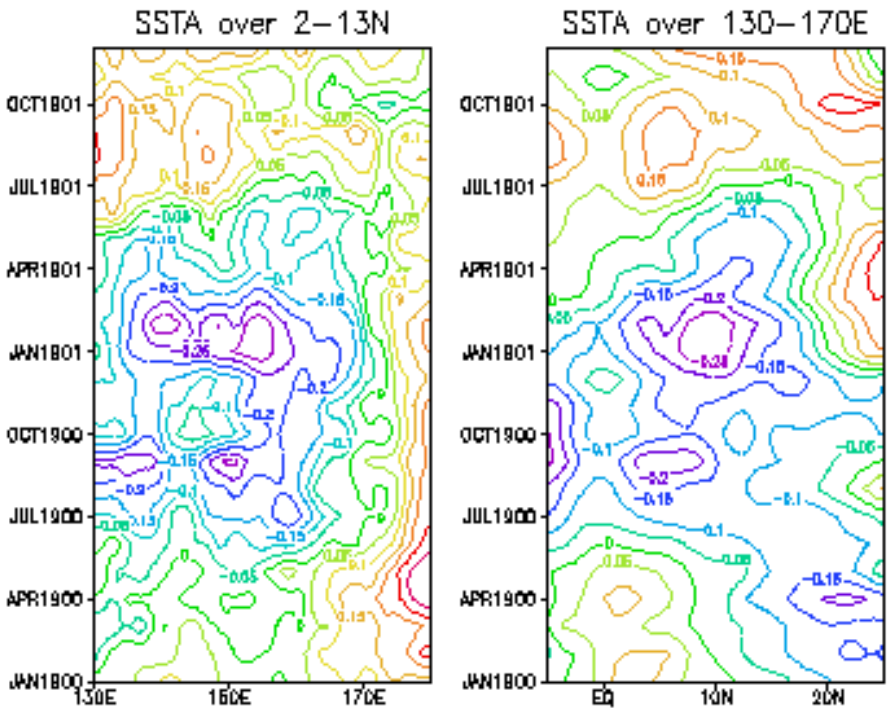

Figure 2. Both hovmuller diagrams show that there are two SST cooling maxima: the first one occurs in August-September of the Nino(0) year, the second in January-February in the Nino(1) year. Data Source: HADISST 1.1.

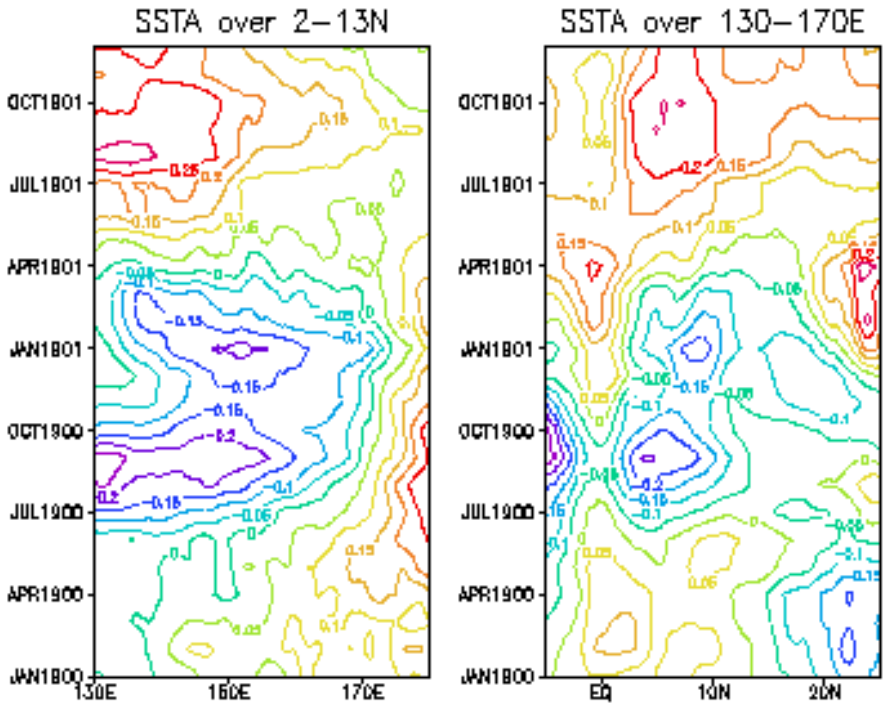

Figure 3. Hovmuller diagrams from OFES show the similar SST evolution with the observation, but a much weaker cooling in January-February in the Nino(1) year.

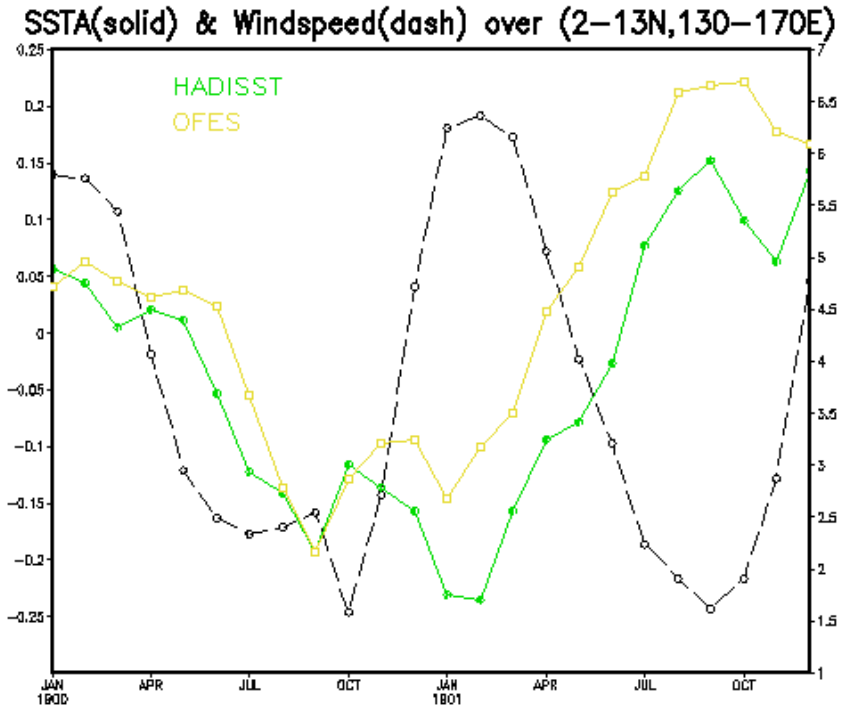

Figure 4. Time series of the composite monthly wind speed field as well as the SSTA from Hadisst and OFES averaged over the western Pacific region.

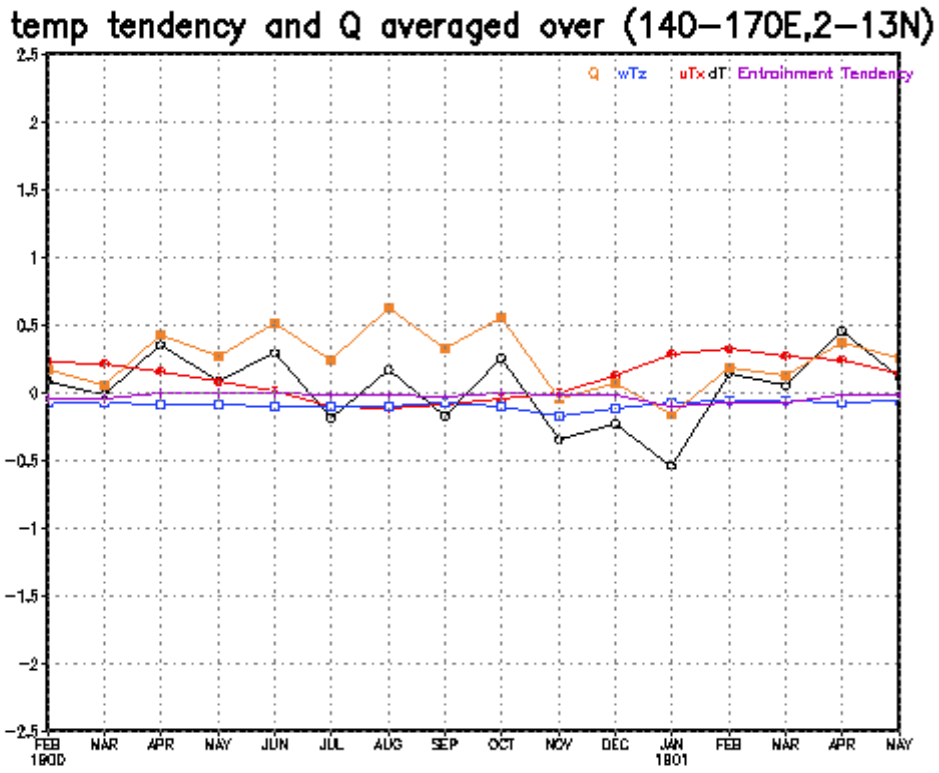

Figure 5. Time series of the composite monthly heat budget over the western Pacific region from OFES

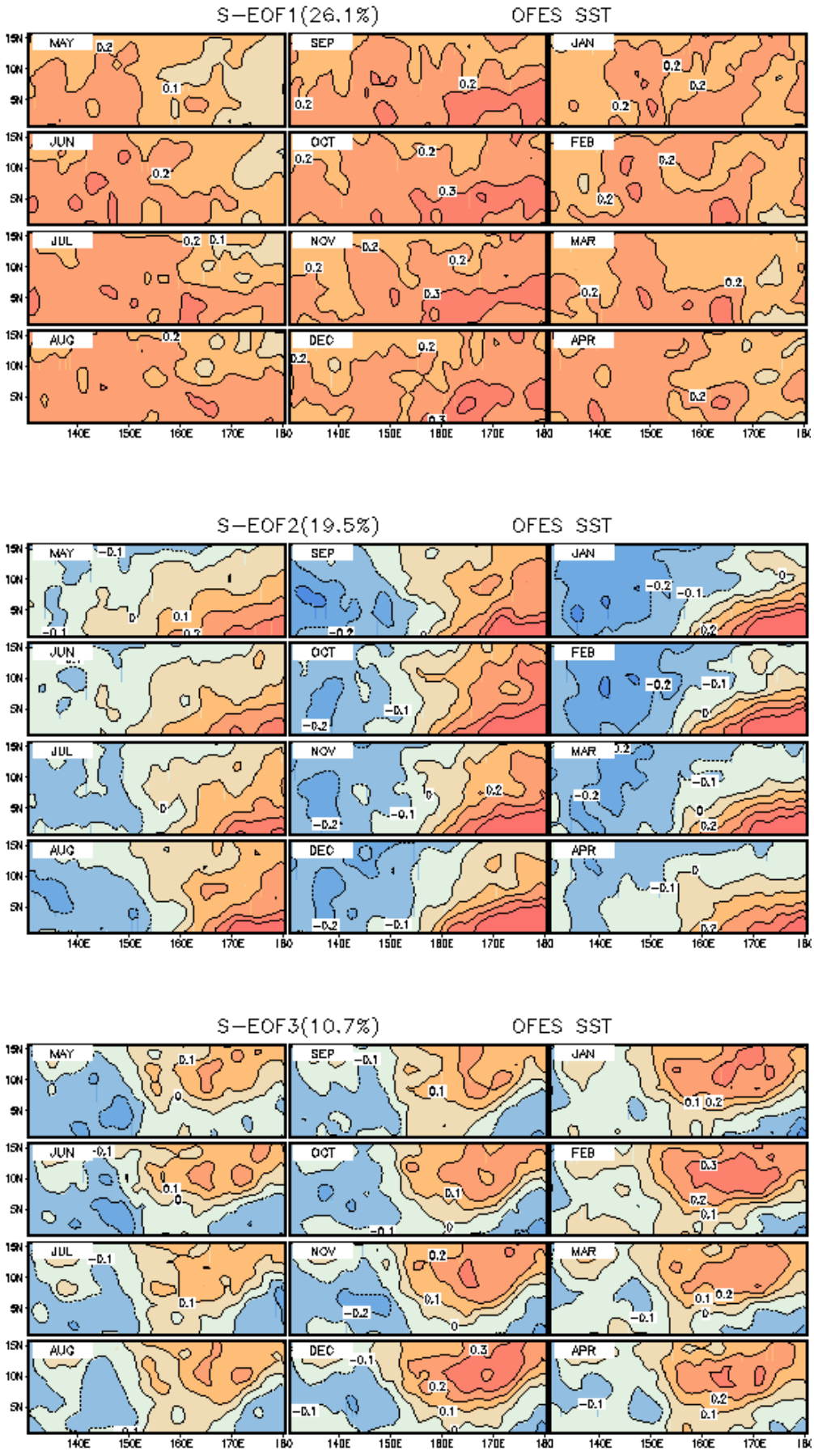

Figure 6. S-EOF analysis of monthly mean SST during 1955-2003 period. The percentage of each mode of total variance is in the parenthesis.

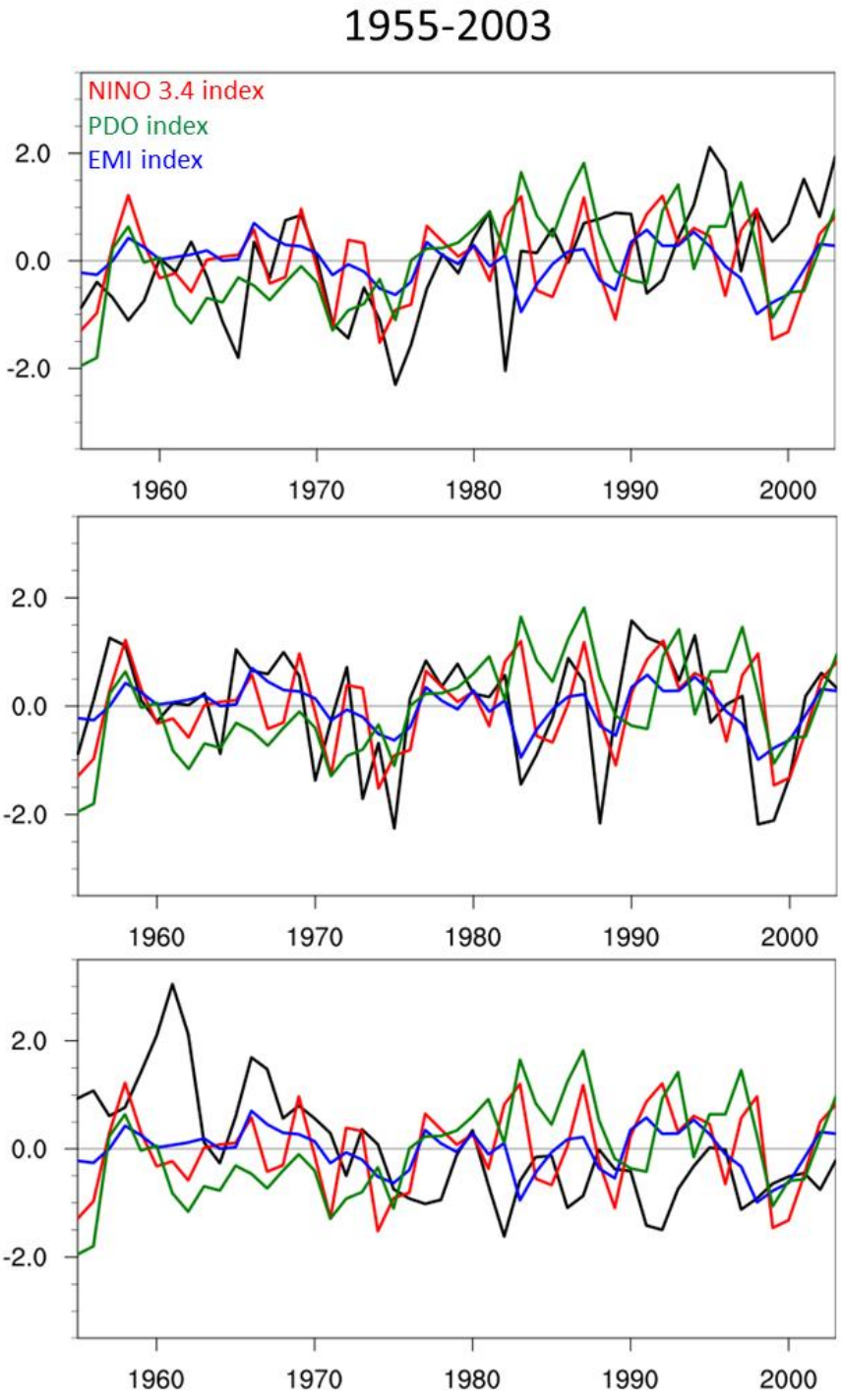

Figure 7. Time series of each S-EOF mode (black line) as well as Nino3.4, EMI and PDO indices.

	pc1				pc2				pc3			
	NINO3	NINO3.4	EMI	PDO	NINO3	NINO3.4	EMI	PDO	NINO3	NINO3.4	EMI	PDO
-5	-0.17	-0.21	-0.24	0.06	-0.01	-0.01	-0.08	-0.04	-0.43	-0.34	0.13	0.08
-4	0.05	-0.03	-0.21	0.02	-0.04	-0.08	-0.13	0.09	-0.17	-0.11	0.01	-0.04
-3	0.26	0.16	-0.27	-0.05	-0.16	-0.16	-0.09	-0.06	0.05	0.10	0.07	0.06
-2	0.24	0.17	-0.17	0.00	0.01	0.07	0.10	0.06	-0.06	0.04	0.20	-0.04
-1	-0.07	-0.08	0.09	-0.03	0.65	0.79	0.66	-0.09	-0.40	-0.29	0.25	0.09
0	0.11	0.10	0.10	-0.02	0.26	0.40	0.76	0.07	-0.33	-0.23	0.21	-0.05
1	0.25	0.22	0.14	0.00	-0.37	-0.23	0.31	0.02	-0.01	0.08	0.23	0.03
2	0.13	0.12	0.01	-0.03	-0.17	-0.13	0.08	-0.02	0.06	0.18	0.30	-0.04
3	0.25	0.22	0.02	0.01	0.03	0.00	-0.16	-0.07	-0.01	0.11	0.37	0.04
4	0.22	0.18	-0.10	0.03	0.11	0.05	-0.18	-0.01	-0.19	-0.12	0.17	-0.02
5	0.14	0.07	-0.30	-0.01	-0.21	-0.24	-0.15	-0.03	-0.34	-0.31	-0.09	0.02

Table 1. Lag correlation of each PC and various climate indices